Research Article

Optimization with Genetic Algorithm of Linear Quadratic Regulator Controller for Active Trailer Braking System

Ali Tahir Karasahin [1*], Mehmet Karali[2]

[1*] Mechatronics Engineering Department, University of Karabük, Karabük, Turkey
(ORCID: 0000-0002-7440-1312), tahirkarasahin@karabuk.edu.tr
[2] Mechatronics Engineering Department, University of Necmettin Erbakan, Konya, Turkey
(ORCID: 0000-0002-2380-0575), mkarali@erbakan.edu.tr
[*] Correspondence: tahirkarasahin@karabuk.edu.tr

(First received February 27, 2022 and in final form June 06, 2022)

Reference: Karaşahin, A. T., & Karali, M. Optimization with Genetic Algorithm of Linear Quadratic Regulator Controller for Active Trailer Braking System. *The European Journal of Research and Development*, *2*(2), 1–12.

Abstract

The necessity of active chassis control methods that can cope with the three typical unstable motion modes found in vehicle-trailer systems has emerged. Although there are studies aimed at preventing these instability situations mechanically, they cannot guarantee lateral stability. Active trailer braking system (ATBS) is used to solve this problem. In this study, a linear quadratic regulator (LQR) to be developed for the car-trailer system. The parameters of LQR are determined using the genetic algorithm (GA). The controller is developed in MATLAB/Simulink and experimentally validated in CarSim. It has been observed that the parameters to be determined by the genetic algorithm give better results than the parameters found by the trial-and-error method.

Keywords: Active trailer braking, Lateral stability, LQR controller

1. Introduction

The dynamics of articulated vehicles differ according to the dynamics of other vehicles [1]–[4]. Especially at high speeds, unstable movement modes occur in vehicle-trailer systems. These; It is expressed as the trailer's sliding, overturning, and trailer folding [5]. In case of sudden maneuvering, while driving, various accidents and injuries can occur due to these unstable modes [6]. If there is no active chassis controller in the vehicle-trailer system, what the drivers can do during this maneuver is limited.

Various studies are carried out to increase the stability of vehicle-trailer systems. They obtained results testing the stability of the vehicle-trailer system using active trailer braking with different axles and centers of gravity. Dynamic and static stability analysis of car-trailer systems were carried out. Critical speeds of the specified systems have been determined. As an active control technique: symmetric braking and differential braking were used. The effectiveness of control techniques has been demonstrated under various test maneuvers [7]. They demonstrated the effect of different active chassis control techniques on lateral stability. The comparative results of the Active Trailer Braking, Active Trailer Steering Control, and Variable Geometry Approach techniques show their superiority over each other. At the same time, the LQR controller is designed and its advantages against the non-controller situation are expressed with the simulation results [8].

It used the Active Trailer Braking system to increase the lateral stability of the vehicle-trailer system. The system is expressed in three degrees of freedom model. An LQR controller is designed. The stability of the controller has been tested with a single lane-change maneuver. With the LQR controller, the lateral stability of the vehicle-trailer system at high speeds is improved[9]. The effect of dynamic models with different degrees of freedom in vehicle-trailer systems has been studied. Vehicle-trailer system; It is expressed in linear 3 degree-of-freedom (DOF), non-linear 4 DOF, non-linear 6 DOF, and CarSim models. According to the tests carried out, it was stated that while 3 DOF produced similar results with other models in low lateral acceleration maneuver, poor results were obtained compared to other models during high lateral acceleration maneuver[10].

LQR and H_∞ controllers were designed to improve the lateral stability of car-trailer systems. The developed controllers are modeled with 3 and 5 DOFs. The stability of the car-trailer systems is improved with the robust controller design against the uncertainties of the parameters. Optimal control parameters for the active chassis control system were determined by genetic algorithm. As a result of experimental studies, it has been shown with the proposed controller that the stability of car-trailer systems can be improved effectively [11].

Different control strategies have been proposed to improve the lateral stability of car-trailer systems. With different linear and nonlinear degrees of freedom, the car-trailer system has been tested under different scenarios. As a result of the tests, it was shown that the dynamic responses of the linear model were within the acceptable range at low lateral acceleration (less than 0.5g) maneuver. However, it was stated that the nonlinear model exhibits more accurate dynamic behaviors in cases of high lateral acceleration [12].

A model predictive controller (MPC) based controller has been developed to prevent unstable modes from occurring in car-trailer systems. The developed controller controls the yaw rate and articulation angle. The effect of differential braking has been

tested under different scenarios. The results obtained have shown that the developed controller is successful against unstable modes [13].

2. Materials and Methods

To improve the lateral stability of car-trailer systems, an LQR-based controller with optimized parameters will be developed with GA. First, dynamic motion equations of the car-trailer system will be derived. The equations obtained will be linearized with the specified conditions. A cost-based LQR control technique will be applied to the car-trailer system in linear systems. LQR controller parameters will be determined with GA. Their performances will be compared with the results obtained by the trial-and-error method.

2.1.Modelling

In this section, the car-trailer system will be expressed with a 3 degree of freedom linear model [8] and its dynamic behavior will be examined. Car-trailer free-body diagram is shown in Figure 1.

Degrees of freedom of 3 degrees of freedom linear model:

- V – vehicle lateral speed (m/s)
- r – vehicle yaw rate (rad/s)
- ψ – articulation angle (rad)

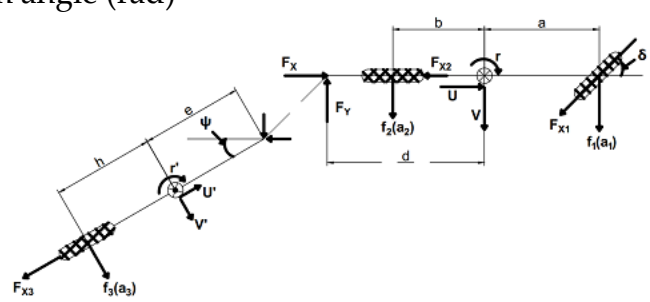

Figure 1 The free-body diagram of a 3 degree of freedom vehicle model

While obtaining the equations of motion, it is assumed that the pairs of wheels in each axle have the same slip angle. Vehicle equations of motion,

$$m_1(\dot{U} - V.r) = -F_{X1}.cos\delta - F_{X2} + F_X \tag{1}$$

$$m_1(\dot{V} - U.r) = f_1(a_1) + f_2(a_2)\delta + F_{X1}.sin\delta - F_Y \tag{2}$$

$$I_1\dot{r} = a.f_1(a_1) - b.f_2(a_2) + a.F_{X1}.sin\delta + d.F_Y \tag{3}$$

Equations of motion for trailer,

$$m_2(\dot{U}' - V'.r') = -F_{X3} - F_X.cos\psi - F_Y.sin\psi \tag{4}$$

$$m_2(\dot{V}' - U'.r') = f_3(a_3) - F_X.sin\delta + F_Y.cos\psi \tag{5}$$

$$I_2\dot{r'} = -h.f_3(a_3) - e.F_X.sin\psi + e.F_Y.cos\psi \tag{6}$$

The vehicle and trailer are connected by the articulation point and their speed and acceleration at this point are equal. While obtaining the equations of motion of the trailer, a fixed coordinate system that takes the center of gravity of the vehicle as a reference is used. In this case, for the longitudinal and lateral speeds of the trailer,

$$U' = U.cos\psi - (V - dr)sin\psi \tag{7}$$

$$V' = U.sin\psi + (V - dr)cos\psi - e.r' \tag{8}$$

equations can be written. As can be understood from the vehicle and trailer Equation (1)-(6) motion equations, a nonlinear equation set is used. To obtain the linear equation of motion:

- The longitudinal speed $U(t)$ is a constant. Equation (1) is ignored.
- Small angle approximations $cos\psi = 1, sin\psi = \psi$ acceptable.
- For initial conditions,

$$\dot{\psi} = r - r' \tag{9}$$

- All dependent variables are ignored.

If the lateral wheel force is expressed using the linear equation of the wheel slip angle, for each wheel,

$$f_i(a_i) = C_i a_i \tag{10}$$

It can be expressed as,

$$a_1 = \frac{V + ra}{U} - \delta_f \tag{11}$$

$$a_2 = \frac{V - rb}{U} \tag{12}$$

$$a_3 = \frac{[V - r(d + e + h) + (e + h)\dot{\psi}]}{U} + \psi \tag{13}$$

Equations can be used for each wheel. Equation sets that we can express the state variables have been obtained by writing their places in the equations written between Equation (1) – (6) [14]. When the equations of motion are linearized under the conditions mentioned above, it can be expressed with the state-space representation below.

$$M\{\dot{x}\} + D\{x\} + F\delta = 0 \tag{14}$$

State variable as,

$$\{x\} = \{V\ r\ \dot{\psi}\ \psi\} \tag{15}$$

M, D and F matrices are specified in the appendix. Physical parameters of the vehicle and trailer are shown in Table 1.

Table 1 Parameters and Definitions

Parameters	Description	Value	Unit
m_1	Car mass	2034	kg
I_1	Car yaw inertia	4605	kgm^2
a	Car dimension	1.835	m
b	Car dimension	1.385	m
d	Car dimension	2.37	m
m_2	Trailer mass	1175	kg
I_2	Trailer yaw inertia	2496	kgm^2
e	Car dimension	3.193	m
h	Car dimension	0.063	m
C_1	Cornering stiffness of car front tires	-75000	Nm/rad
C_2	Cornering stiffness of car rear tires	-75000	Nm/rad
C_3	Cornering stiffness of trailer tires	-60000	Nm/rad

2.2. Active Trailer Differential Braking System

Three degrees of freedom equations of the vehicle-trailer system have been obtained. The motion equations obtained for the active trailer differential braking (ATDB) system need to be rearranged. ATDB system only affects Equation (6). With the ATDB application, an extra $\boldsymbol{\Delta M_z}$ moment is added to the trailer [7].

$$I_2\dot{r'} = -h.f_3(a_3) - e.F_X.sin\psi + e.F_Y.cos\psi + \Delta M_z \tag{16}$$

When the equations of motion for the ATDB system are rearranged, the state-space representation also changes.

$$M\{\dot{x}\} + D\{x\} + C_b u + F\delta = 0 \tag{17}$$

$$u = \Delta M_z \tag{18}$$

M, D, and F matrices that express the vehicle model will remain the same. $\boldsymbol{C_b}$ added to the moment equation is the control matrix and is specified in the appendix.

2.3. Controller Design

Controller design will be carried out with the LQR technique [15] to evaluate the lateral stability of the car-trailer system. Controller design will be implemented for a system defined by state-space representation. The state-space form for the ATDB system is shown in Equation (17). LQR technique is a design method in which all situations are evaluated with feedback and a relationship can be established between inputs and outputs of the system. Input signals to be applied to the system in full state feedback or pole placement technique can be inapplicable. The signals to be applied to the system can be reduced to applicable sizes by entering the system with the optimization approach in the LQR technique. The performance index used in the LQR control technique is shown in Equation (19).

$$J = \int_0^\infty (x^t\,(t)Qx(t) + u^t Ru(t))dt \tag{19}$$

$\boldsymbol{U(t)}$ is the control input specified in Equation (19), $\boldsymbol{x(t)}$ is the state variables specified in equation (15), and $\boldsymbol{Q}$ and $\boldsymbol{R}$ are the weight matrices. If all situations are assumed to be stable, the solution to the optimization problem is determined as the controller response to be applied to the CT system. The controller input is calculated as expressed in equation (20). Here $\boldsymbol{K}$ matrix refers to the feedback control matrix.

$$u = -Kx(t) \tag{20}$$

The trial-and-error method is generally used to determine the parameters of the LQR controller. This process costs time for designers. However, it cannot be guaranteed that the parameters obtained will give the best results. At this point, optimization algorithms that work with the best result search approach come into play. Thus, it can be guaranteed that the determined parameters will produce the best results.

2.4. Genetic Algorithm

Genetic algorithm (GA), one of the search algorithms, is trying to give the best result in the optimization problem. It was proposed by John Holland in 1975. GA operators consist of selection, mutation, and crossover. It is classified as a population-based optimization algorithm. It works to optimize the fitness function determined by the designer. It achieves the best result by transferring strong individuals in the population to the next generations. GA flow diagram is given in Figure 2.

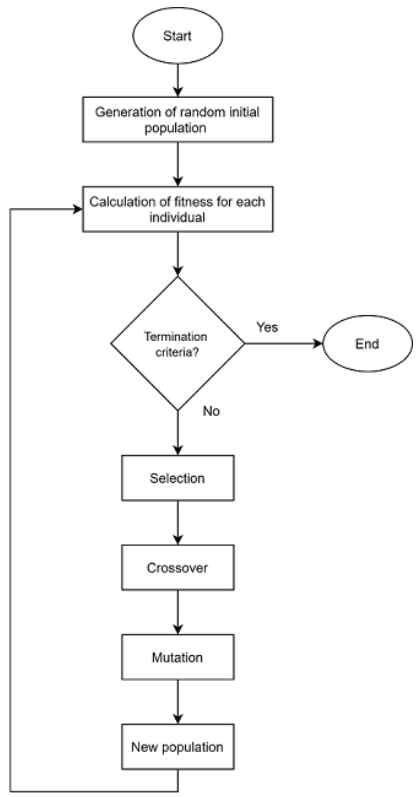

Figure 2 Genetic algorithm flow diagram

3. Results

Various studies have been carried out to determine the parameters of the LQR controller used in car-trailer systems by optimization algorithms [11]. In the study carried out, the values of the degrees of freedom of the 3 DOF model will be minimized by comparing the controller with active and passive control. LQR controller weight function is shown in Equation (21).

$$Q = diag([q1\ q2\ q3\ q4]), R = [r] \tag{21}$$

The fitness function in GA is indicated in Equation (22).

$$f_{obj} = \frac{\phi_1}{\phi_1^p} + \frac{\phi_2}{\phi_2^p} + \frac{\phi_3}{\phi_3^p} \tag{22}$$

$\boldsymbol{\phi_1}, \boldsymbol{\phi_2}, \boldsymbol{\phi_3}$ when the ATDB controller is active, the lateral velocity of the vehicle, the yaw rate of the vehicle, the angle of articulation, refers to the value of the degrees of freedom arranged with Root of Mean Square (RMS). $\boldsymbol{\phi_1^p}, \boldsymbol{\phi_2^p}, \boldsymbol{\phi_3^p}$ denote the RMS of the value of degrees of freedom when the control is passive. In this study, the performance of the controller will be tested with the double lane change maneuver specified in ISO 3888-1. The ISO 3888-1 maneuver applied at a speed of 90 km/h in the CarSim environment is shown in Figure 3.

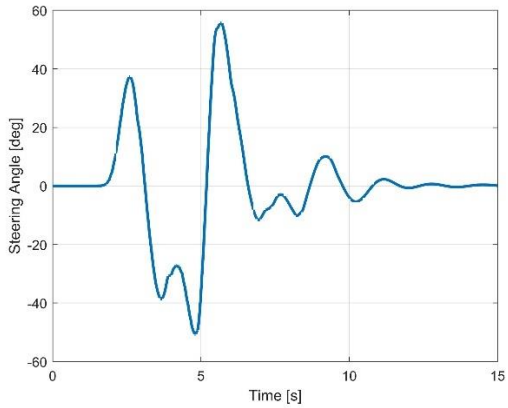

Figure 3 Double lane change maneuver

Thanks to the lane change maneuver applied, the LQR controller performances determined by the trial-and-error method and optimized with GA were compared. In Figure 4, the GA optimized LQR controller has a maximum yaw rate of 17.85 deg/s, while the LQR controller whose coefficients are determined by trial-and-error method has a maximum yaw rate of 18.05 deg/s.

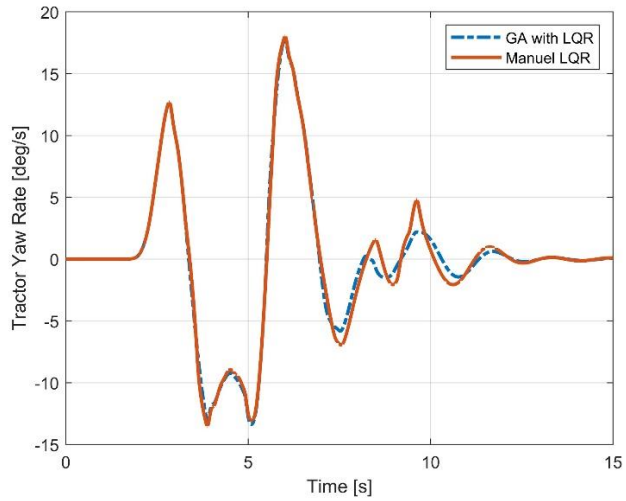

Figure 4 Compare of LQR controller performance for tractor yaw rate

In Figure 5, the GA-optimized LQR controller observed a maximum lateral velocity of 2.03 m/s, while the manual LQR controller recorded a maximum lateral velocity of 2.05 m/s.

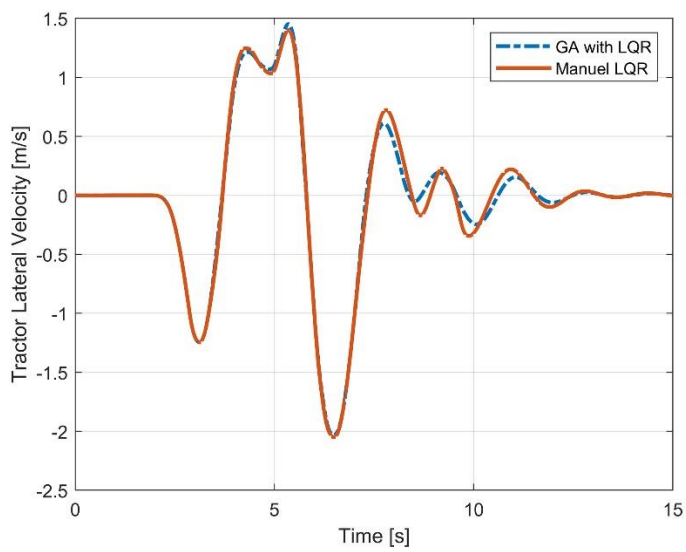

Figure 5 Compare of LQR controller performance for tractor lateral velocity

In Figure 6, a maximum hitch angle of 10.4 deg was observed in the GA optimized LQR controller, while a maximum hitch angle of 10.3 deg was recorded in the manual LQR controller.

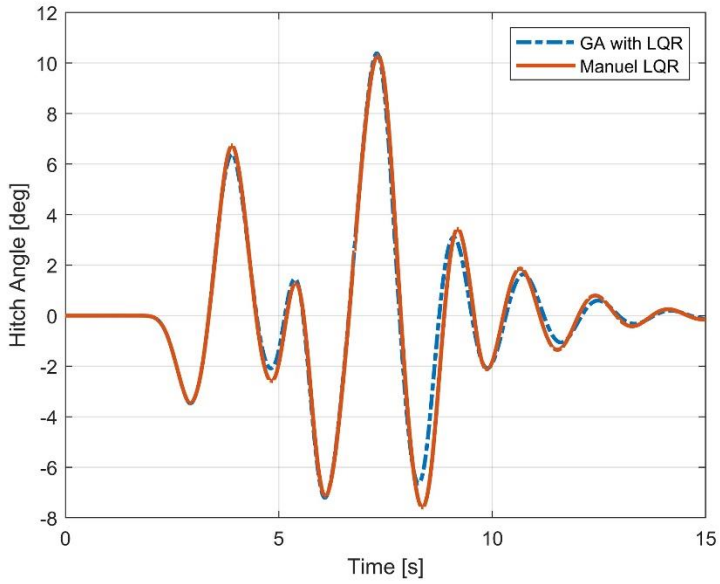

Figure 6 Compare of LQR controller performance for hitch angle

In Figure 7 the braking torque to be applied by the controller is limited to 600 N.m. In this case, it has been observed that the GA-optimized LQR controller needs less braking torque.

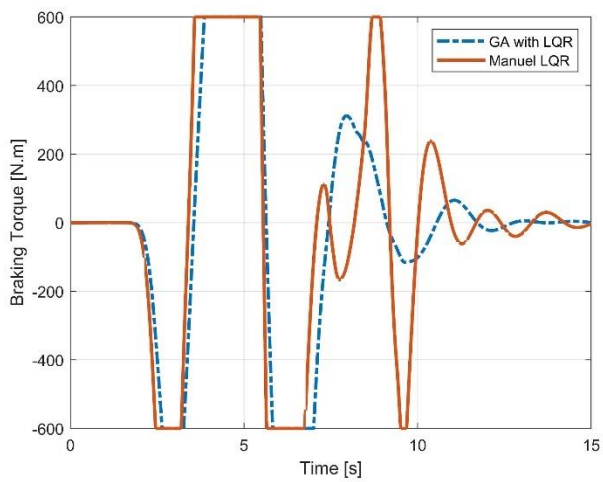

Figure 7 Control response of car-trailer system

4. Discussion and Conclusion

The car-trailer system was modeled with 3 DOFs and dynamic motion equations were obtained. The equations obtained are linearized under certain assumptions. LQR controller was designed according to the dynamic model obtained. The Q and R weight

matrices are GA optimized. To test the performance of the LQR controller, an ISO 3888-1 double lane change maneuver at a speed of 90 km/h was applied. As a result of experiments carried out in CarSim and MATLAB-Simulink environments, the LQR controller has been successful in improving the stability of the car-trailer system. The trailer behaved erratically while the controller was off, and this was eliminated when the controller was activated. The GA-optimized LQR controller was more successful than the LQR controller whose coefficients were determined by the trial-and-error method.

References

[1] X. Kang and W. Deng, "Vehicle-trailer handling dynamics and stability control - An engineering review," 2007. doi: 10.4271/2007-01-0822.

[2] Y. He, H. Elmaraghy, and W. Elmaraghy, "A design analysis approach for improving the stability of dynamic systems with application to the design of car-trailer systems," *Journal of Vibration and Control*, vol. 11, no. 12, pp. 1487–1509, 2005.

[3] J. Darling, D. Tilley, and B. Gao, "An experimental investigation of car—trailer high-speed stability," *Proceedings of the Institution of Mechanical Engineers, Part D: Journal of Automobile Engineering*, vol. 223, no. 4, pp. 471–484, 2009.

[4] Y. Zhao, S. Chen, and T. Shim, "Investigation of trailer yaw motion control using active front steer and differential brake," *SAE International Journal of Materials and Manufacturing*, vol. 4, no. 1, pp. 1057–1067, 2011.

[5] X. Yang, J. Song, and J. Gao, "Fuzzy logic based control of the lateral stability of tractor semitrailer vehicle," *Mathematical Problems in Engineering*, vol. 2015, 2015.

[6] NHTSA, "2017 Fatal Motor Vehicle Crashes: Overview." 2020.

[7] A. Hac, D. Fulk, and H. Chen, "Stability and control considerations of vehicle-trailer combination," *SAE International Journal of Passenger Cars-Mechanical Systems*, vol. 1, no. 2008-01–1228, pp. 925–937, 2008.

[8] R. Shamim, M. M. Islam, and Y. He, "A comparative study of active control strategies for improving lateral stability of car-trailer systems," 2011.

[9] T. Sun, Y. He, E. Esmailzadeh, and J. Ren, "Lateral stability improvement of car-trailer systems using active trailer braking control," *Journal of Mechanics Engineering and Automation*, vol. 2, no. 9, pp. 555–562, 2012.

[10] Y. He and J. Ren, "A Comparative Study of Car-Trailer Dynamics Models," *SAE International Journal of Passenger Cars - Mechanical Systems*, vol. 6, no. 1, pp. 177–186, 2013, doi: 10.4271/2013-01-0695.

[11] E. Lee, "Design Optimization of Active Trailer Differential Braking Systems for Car-Trailer Combinations," 2016.

[12] T. Sun, "Design Synthesis of Car-Trailer Systems with Active Trailer Differential Braking Strategies," 2013. Accessed: Sep. 11, 2020. [Online]. Available: https://ir.library.dc-uoit.ca/xmlui/bitstream/handle/10155/350/Sun_Tao.pdf?sequence=1

[13] M. Abroshan, R. Hajiloo, E. Hashemi, and A. Khajepour, "Model predictive-based tractor-trailer stabilisation using differential braking with experimental verification," *Vehicle System Dynamics*, pp. 1–24, 2020.

[14] X. Ding, Y. He, J. Ren, and T. Sun, "A comparative study of control algorithms for active trailer steering systems of articulated heavy vehicles," in *2012 American Control Conference (ACC)*, 2012, pp. 3617–3622.

[15] J. P. Hespanha, "Topics in Undergraduate Control Systems Design." 2012.

Appendix

$$M = \begin{bmatrix} m_1 + m_2 & -m_2 d & -m_2 e & 0 \\ -m_2 d & I_1 + m_2 d^2 & m_2 e d & 0 \\ -m_2 e & m_2 e d & I_2 + m_2 e^2 & 0 \\ 0 & 0 & 0 & 1 \end{bmatrix}$$

$$D = \frac{1}{u}\begin{bmatrix} -c_1 - c_2 - c_3 & -c_1 a + c_2 b + c_3 d + (m_1 + m_2)u^2 & c_3(h+e) & -c_3 u \\ -c_1 a + c_2 b + c_3 d & -c_1 a^2 - c_2 b^2 - c_3 d^2 - m_2 d u^2 & -c_3 d(h+e) & c_3 d u \\ c_3(h+e) & -c_3 d(h+e) - m_2 e u^2 & -c_3(h+e)^2 & c_3(h+e)u \\ 0 & -u & u & 0 \end{bmatrix}$$

$$F = \begin{bmatrix} c_1 \\ c_1 a \\ 0 \\ 0 \end{bmatrix}, \quad C_b = \begin{bmatrix} 0 \\ 0 \\ -1 \\ 0 \end{bmatrix}$$

$$K_{man} = 1.0e + 03 * [-0.4569 \quad 3.6058 \quad -1.6029 \quad 1.2321]$$

$$K_{GA} = 1.0e + 03 * [-0.4779 \quad 2.3416 \quad -0.2545 \quad 1.9084]$$